

$^{233}\text{Pa}(n, \gamma)$ cross section extraction using the surrogate reaction $^{232}\text{Th}(^3\text{He}, p)^{234}\text{Pa}^*$ involving spin-parity distribution

C. X. Tan (谭畅翔),¹ X. X. Li (李鑫祥),^{1,*} D. Y. Pang (庞丹阳),² W. D. Chen (陈文棣),²
J. G. Chen (陈金根),³ C. Z. Shi (施晨钟),³ and W. Luo (罗文),^{1,†}

¹*School of Nuclear Science and Technology, University of South China, 421001 Hengyang, China*

²*School of Physics, Beihang University, 100191 Beijing, China*

³*Shanghai Institute of Applied Physics, Chinese Academy of Sciences, 201800 Shanghai, China*

 (Received 22 December 2023; revised 7 March 2024; accepted 28 March 2024; published 17 April 2024)

The neutronic properties of ^{233}Pa play a crucial role in the thorium fuel cycle since it directly impacts the inventory of the fissile isotope ^{233}U . Currently, the experimental data of the $^{233}\text{Pa}(n, \gamma)$ cross section are rather scanty with poor accuracy and significant discrepancy exists in the experimental and evaluated data. In this work, the $^{233}\text{Pa}(n, \gamma)$ cross section is studied through the surrogate reaction $^{232}\text{Th}(^3\text{He}, p)^{234}\text{Pa}^*$. The spin-parity (SP) distribution of the $^{232}\text{Th}(^3\text{He}, p)^{234}\text{Pa}^*$ is calculated with the distorted wave Born approximation and then the $^{233}\text{Pa}(n, \gamma)$ cross section is extracted using the statistical Hauser-Feshbach model. It is found that the extracted $^{233}\text{Pa}(n, \gamma)$ data considering the SP distribution have a tendency to agree with the evaluated nuclear data files, ENDF/B-VIII.0 and JENDL-5, whereas the experimental ones without considering the SP distribution are visibly higher than the evaluated data. This suggests that the SP distribution should be considered reasonably when employing the surrogate-reaction method to extract the $^{233}\text{Pa}(n, \gamma)$ cross section.

DOI: [10.1103/PhysRevC.109.044615](https://doi.org/10.1103/PhysRevC.109.044615)

I. INTRODUCTION

There is an increasing interest in molten salt reactors (MSR) both from industry and academia because of the potential advantages in terms of safety, sustainable fuel cycle, high melting and boiling points of salt, and efficient electrical power generation [1–3]. Liquid fueled MSR are often associated with the ^{232}Th - ^{233}U fuel cycle. In this fuel cycle the fissile nucleus ^{233}U is generated by neutron capture of fertile nucleus ^{232}Th and two successive β^- decays. The production of ^{233}U is governed by the 26.98 d half-life of ^{233}Pa and the inventory of the fissile material ^{233}U will depend strongly on the neutronic properties of the intermediate ^{233}Pa . Neutron capture in ^{233}Pa is a twofold loss involving both the loss of an otherwise useful neutron and a potential nucleus ^{233}U . The medium long-life of ^{233}Pa makes the (n, γ) cross section of this nucleus important to the operation and neutron economy of the MSR system [4].

Experimental data on the $^{233}\text{Pa}(n, \gamma)$ cross section are rather scanty and discrepant or missing [5–8]. Most of these data have only one value in the thermal energy range. There exists a great challenge in direct measurement of the $^{233}\text{Pa}(n, \gamma)$ cross section because of the medium half-life (26.98 d) and high specific activity ($\approx 10^9$ Bq/g) of the ^{233}Pa . Surrogate reaction seems to be an alternative method to investigate the (n, γ) cross section on rare and unstable nuclei [9]. In 2006, Boyer *et al.* measured the γ -decay probability $P_{\delta\gamma}(E^*)$ of the surrogate reaction $^{232}\text{Th}(^3\text{He}, p)^{234}\text{Pa}^*(P_{\text{exp}})$,

and then obtained the $^{233}\text{Pa}(n, \gamma)$ cross section up to neutron energies of 1 MeV. The uncertainty of the $^{233}\text{Pa}(n, \gamma)$ cross section varies from 7% at the neutron energy of $E_n = 0.1$ MeV to 21% at $E_n = 0.9$ MeV [10]. On the one hand, Boyer's data are almost two times higher than the values provided by the ENDF/B-VIII.0 [11] and the JENDL-5 [12], where the data of ENDF/B-VIII.0 are deduced from fitting the $^{231}\text{Pa}(n, f)$ experimental data [13] and the JENDL-5 evaluations are based on a statistical model calculation [14]. On the other hand, the Boyer's data have up to four times difference compared to the ROSFOND-2010 evaluations [15], which are extrapolated from (n, γ) cross sections of neighboring nuclei (^{232}Th , ^{235}U , and ^{238}U). Note that the γ -decay probability strongly depends on spin-parity (SP) distribution, which corresponds to the probabilities that the compound nucleus is formed in the SP state by the surrogate reaction. The SP mismatch can lead to important deviations between the neutron-induced data and the ones obtained with the surrogate-reaction method [16]. Since Boyer's data did not include the SP effect in the surrogate reaction $^{232}\text{Th}(^3\text{He}, p)^{234}\text{Pa}^*$ [17], it is worth to investigate the impact of the SP effect on the $^{233}\text{Pa}(n, \gamma)$ cross section obtained using surrogate-reaction method, and then to resolve the significant discrepancy between the available experimental data and the evaluated ones.

In this study, we propose to extract the $^{233}\text{Pa}(n, \gamma)$ cross section using the surrogate reaction $^{232}\text{Th}(^3\text{He}, p)^{234}\text{Pa}^*$ including the SP effect. The formation cross section for the compound nucleus (CN) $^{234}\text{Pa}^*$ is calculated, which is a necessity for obtaining the $^{233}\text{Pa}(n, \gamma)$ cross section. The SP distribution of the surrogate reaction $^{232}\text{Th}(^3\text{He}, p)^{234}\text{Pa}^*$ is then calculated. By utilizing the χ^2 test, an optimal normalization factor of the γ strength function (γSF) is obtained

*Corresponding author: lixinxiang@usc.edu.cn

†Corresponding author: wenluo-ok@163.com

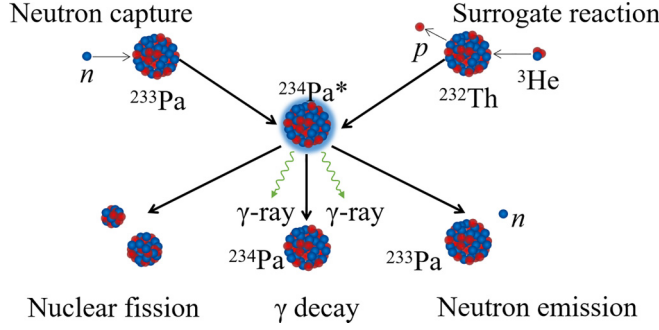


FIG. 1. Schematic representation of the desired reaction $^{233}\text{Pa}(n, \gamma)^{234}\text{Pa}^*$ and surrogate reaction $^{232}\text{Th}(^3\text{He}, p)^{234}\text{Pa}^*$. Generally, the ^{234}Pa decays through the following pathways: nuclear fission, γ decay, and neutron emission with certain probabilities.

and then implemented into the TALYS calculations to extract the $^{233}\text{Pa}(n, \gamma)$ cross section. The remainder of the paper is organized as follows. The surrogate-reaction method used to extract the $^{233}\text{Pa}(n, \gamma)$ cross section is introduced in Sec. II. The results in terms of the formation cross section for the $^{233}\text{Pa}(n, \gamma)^{234}\text{Pa}^*$ reaction, the SP distribution probability for the $^{232}\text{Th}(^3\text{He}, p)^{234}\text{Pa}^*$ reaction and the extracted $^{233}\text{Pa}(n, \gamma)$ cross section are introduced in Sec. III. Finally, a conclusion and perspectives is given in Sec. IV.

II. EXTRACTION METHOD OF $^{233}\text{Pa}(n, \gamma)$ CROSS SECTION

The surrogate-reaction method is an indirect method for determination of the reaction cross section. This method creates the desired CN through alternative (“surrogate”) reaction involving a combination of projectile and target that are more easily achieved in modern physics experiments. It is of great significance for the cases of unstable nuclei [18–23]. In the $^{233}\text{Pa}(n, \gamma)$ reaction, the projectile (n) and the target (^{233}Pa) fuse to form a highly excited $^{234}\text{Pa}^*$, which subsequently de-excites through nuclear fission, γ decay, and neutron emission, which is schematically shown in Fig. 1.

A. Cross section of the $^{233}\text{Pa}(n, \gamma)$ reaction

According to the Bohr hypothesis, the CN completely loses memory of its incident channel, that is, the formation and decay of the CN are independent to each other [24]. The resulting CN system has a transient statistical equilibrium. In consideration of the conservation of angular momentum J and parity π , the CN reactions can be appropriately described with the statistical Hauser-Feshbach (HF) model [25], which provides the following expression of the $^{233}\text{Pa}(n, \gamma)$ cross section:

$$\sigma_{n\gamma}(E_n) = \sum_{J, \pi} \sigma_n^{CN}(E^*, J, \pi) G_\gamma^{CN}(E^*, J, \pi) \times W_{n, \gamma}(E_n, J, \pi), \quad (1)$$

where $\sigma_n^{CN}(E^*, J, \pi) = \sigma^{CN}(n + ^{233}\text{Pa} \rightarrow ^{234}\text{Pa}^*)$ represents the cross section for forming the highly excited $^{234}\text{Pa}^*$ at an excitation energy E^* with angular momentum J and

parity π in the neutron-induced reaction, $G_\gamma^{CN}(E^*, J, \pi) = G_\gamma^{CN}(^{234}\text{Pa}^* \rightarrow ^{234}\text{Pa} + \gamma)$ is the branching ratio corresponding to the $^{234}\text{Pa}^*$ decays via emitting one or more γ rays as discussed later, and $W_{n, \gamma}(E_n, J, \pi)$ is the width fluctuation correction factor with E_n being the neutron kinetic energy. In general, $\sigma_n^{CN}(E^*, J, \pi)$ can be calculated by neutron-nucleus effective interactions (“optical potentials”) with a relative high precision. The E_n and E^* have a relationship

$$E_n = \left(1 + \frac{1}{A}\right)(E^* - S_n), \quad (2)$$

where the factor $(1 + \frac{1}{A})$ takes into account the nuclear recoil energy in the reaction $^{233}\text{Pa}(n, \gamma)$, A is the mass number of the nucleus ^{233}Pa , and S_n is the neutron separation energy.

B. SP distribution of the reaction $^{232}\text{Th}(^3\text{He}, p)^{234}\text{Pa}^*$

The population of desired CN generated by the neutron-induced reaction and the surrogate reaction may differ dramatically. The probability for forming the $^{234}\text{Pa}^*$ in the surrogate reaction $^{232}\text{Th}(^3\text{He}, p)^{234}\text{Pa}^*$ can be expressed as

$$F_\delta^{CN}(E^*, J, \pi) = \frac{\sigma_\delta^{CN}(E^*, J, \pi)}{\sum_{J', \pi'} \sigma_\delta^{CN}(E^*, J', \pi')}, \quad (3)$$

where $\sigma_\delta^{CN}(E^*, J, \pi)$ represents the cross section of the reaction $^{232}\text{Th}(^3\text{He}, p)^{234}\text{Pa}^*$. The calculations of the $F_\delta^{CN}(E^*, J, \pi)$ were performed with the distorted wave Born approximation (DWBA) [26]. Distorted waves of the entrance and exit channels were calculated with the systematic optical model potentials of Pang *et al.* [27] for the $^3\text{He} + ^{232}\text{Th}$ system and of Koning and Delaroche [28] for the $p + ^{234}\text{Pa}$ system. The bound state form factor of deuteron in ^3He was calculated with single particle potential parameters derived from Green function Monte Carlo calculations by Brida *et al.* [29]. The bound state form factor of deuteron in different excited states of ^{234}Pa were approximated with the single particle wave functions of the deuteron cluster in ^{234}Pa , which were calculated with Woods-Saxon potentials. The depths of these Woods-Saxon potentials were adjusted to reproduce the separation energies of the deuteron cluster in ^{234}Pa , and the radius and diffuseness parameters were taken to be $R = 1.25 \times 232^{1/3}$ fm and $a = 0.65$ fm, respectively.

C. Branching ratio for the $^{234}\text{Pa}^*$ γ decay

As mentioned above, the $^{234}\text{Pa}^*$ has the decay pathways including nuclear fission, γ decay, and neutron emission. The branching ratio for the $^{234}\text{Pa}^*$ γ decay $G_\gamma^{CN}(E^*, J, \pi)$ is composed of three well-defined functional forms: the γ transmission coefficient $T_\gamma(E^*, J, \pi)$, the fission transmission coefficient $T_f(E^*, J, \pi)$, and the neutron transmission coefficient $T_n(E^*, J, \pi)$ [30]. An exact expression of the $G_\gamma^{CN}(E^*, J, \pi)$ is given by

$$G_\gamma^{CN}(E^*, J, \pi) = \frac{T_\gamma(E^*, J, \pi)}{T_\gamma(E^*, J, \pi) + T_f(E^*, J, \pi) + T_n(E^*, J, \pi)}. \quad (4)$$

In our study, the $G_\gamma^{CN}(E^*, J, \pi)$ for the $^{234}\text{Pa}^*$ is calculated with the statistical model. The following main ingredients were used to model the γ decay of the $^{234}\text{Pa}^*$. The level densities above the ground states of ^{233}Pa and ^{234}Pa were described using the Gilbert-Cameron formula [31] with the parameters adopted from the recommended values of RIPL 3 [30]. For the fission transmission coefficient, it was assumed that the fission process was determined by a double-humped fission barrier. The fission barrier parameters employed the experimental values [32]. It was assumed that only electric dipole ($E1$) and magnetic dipole ($M1$) transitions contributed to the γ -decay channel. Then the expression of $T_\gamma(E^*, J, \pi)$ reads

$$T_\gamma(E^*, J, \pi) = G_{\text{norm}}[T_{M1}(E^*, J, \pi) + T_{E1}(E^*, J, \pi)], \quad (5)$$

where G_{norm} is a normalization factor for the γ SF [33], and $T_{M1}(E^*, J, \pi)$ and $T_{E1}(E^*, J, \pi)$ are the γ transmission coefficient of $M1$ and $E1$, respectively. The γ SF ($M1$) was described using the Goriely's microscopic Gogny-HFB+QRPA model [34] and the γ SF ($E1$) was determined by the Kopecky-Uhl model. In the Kopecky-Uhl model [33], the energy, strength, and width of giant resonances were calculated using the systematic formulas [35,36]. In our case, the G_{norm} value was adjusted in a reasonable way, aiming to conform the calculated γ -decay probabilities of the $^{234}\text{Pa}^*$ with the available experimental data [10], which will be introduced in detail later.

D. Extraction of the $^{233}\text{Pa}(n, \gamma)$ cross section

The extraction of the $^{233}\text{Pa}(n, \gamma)$ cross section was accomplished with the following four steps. First, the $\sigma_n^{CN}(E^*, J, \pi)$ and $W_{n,\gamma}(E_n, J, \pi)$ were modelled with TALYS software (version 1.96) [37] by invoking the semimicroscopic neutron-nucleus spherical optical model potential (OMP) and the Moldauer expression therein, respectively. Second, the γ -decay probability $P_{\delta\gamma}(E^*)$ was obtained by summing the product of $F_\delta^{CN}(E^*, J, \pi)$ [see Eq. (3)] with $G_\gamma^{CN}(E^*, J, \pi)$ [see Eq. (4)] over angular momentum J and parity π . As a result, the expression of $P_{\delta\gamma}(E^*)$ reads [25]

$$P_{\delta\gamma}(E^*) = \sum_{J,\pi} F_\delta^{CN}(E^*, J, \pi) G_\gamma^{CN}(E^*, J, \pi). \quad (6)$$

Third, the factor G_{norm} was obtained by minimizing the χ^2 , which is defined by

$$\chi^2 = \frac{1}{N} \sum_{E^*} \frac{(P_{\text{theo}} - P_{\text{exp}})^2}{P_{\text{err}}^2}, \quad (7)$$

where P_{theo} and P_{exp} represents theoretical and experimental γ -decay $P_{\delta\gamma}(E^*)$, respectively, and P_{err} is the experimental uncertainty. In the experiment of Boyer *et al.* [10], the number of γ rays was determined by the C_6D_6 liquid scintillator, in which the neutron- γ discrimination was accomplished with the difference in detected pulse shape; the identification between charged particles such as proton, deuteron, triton, and α was performed by a standard telescope (ΔE - E) technique. Two group data, namely the energy spectra of the protons in singles and the energy spectra of the protons in coincidence with γ rays detected by at least one of the C_6D_6

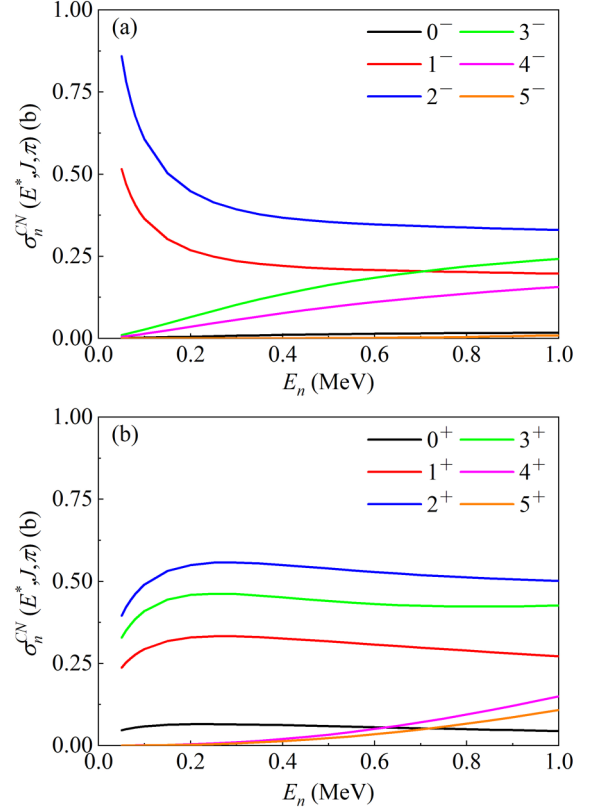


FIG. 2. The calculated $\sigma_n^{CN}(E^*, J, \pi)$ as a function of neutron energy in the cases of negative (a) and positive (b) parities.

scintillators, were then acquired. Accordingly, the experimental neutron capture probabilities were obtained and the experimental γ -decay probabilities of ^{234}Pa (P_{exp}) were further deduced within the excitation energy range 4.92–6.12 MeV. More detailed analyses are presented in Ref. [10]. Although the $^{233}\text{Pa}(n, \gamma)$ cross section $\sigma_n^{CN}(E^*, J, \pi)$ extracted from P_{exp} without considering the SP distribution differs from the evaluated data, the P_{exp} values measured by Boyer *et al.* [10] are the only experimental data so far, which is very important for the theoretical research on the $^{233}\text{Pa}(n, \gamma)$ cross section using the surrogate reaction $^{232}\text{Th}(^3\text{He}, p)^{234}\text{Pa}^*$. By substituting the factor G_{norm} into Eqs. (4) and (5), the $G_\gamma^{CN}(E^*, J, \pi)$ was obtained accordingly. Finally, the $^{233}\text{Pa}(n, \gamma)$ cross section was obtained by substituting the calculated $\sigma_n^{CN}(E^*, J, \pi)$, $W_{n,\gamma}(E_n, J, \pi)$, and $G_\gamma^{CN}(E^*, J, \pi)$ into Eq. (1).

III. RESULTS AND DISCUSSIONS

A. CN formation cross section

Given different negative and positive parities, the simulated $\sigma_n^{CN}(E^*, J, \pi)$ as a function of neutron energy are shown in Fig. 2. The uncertainty is about 5% for the statically deformed nuclei [20]. For the J^- states of $1\hbar$ and $2\hbar$, the $\sigma_n^{CN}(E^*, J, \pi)$ first decrease rapidly and then get flattened. This is because the ^{233}Pa has the ground state $J^- = 3/2\hbar$ and the $^{234}\text{Pa}^*$ populated with relatively low energy neutrons would have priority states of $J^- = 1\hbar$ and $2\hbar$. For other J^-

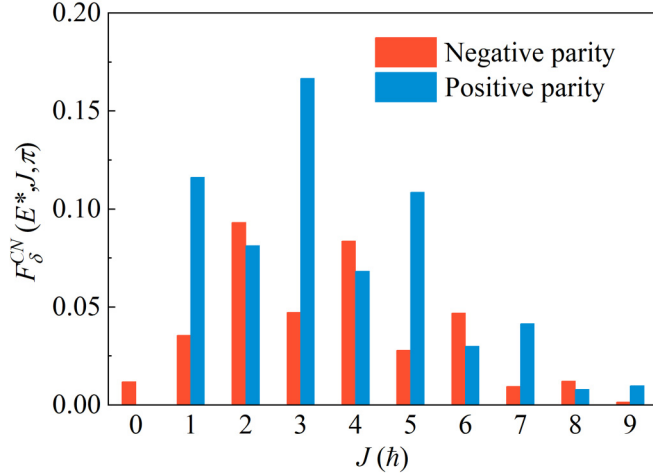


FIG. 3. The calculated $F_{\delta}^{CN}(E^*, J, \pi)$ for $^{234}\text{Pa}^*$ populated by the reaction $^{232}\text{Th}(^3\text{He}, p)$ at 5.72 MeV.

states, the $\sigma_n^{CN}(E^*, J, \pi)$ keep an increasing trend with the neutron energy. For the states $J^+ \leq 3\hbar$, the $\sigma_n^{CN}(E^*, J, \pi)$ increase within the energy range $E_n \leq 0.2$ MeV and then have a slight decrease. Above $J^+ = 3\hbar$, the $\sigma_n^{CN}(E^*, J, \pi)$ show the same tendency with the cases at $J^- = 4\hbar$ and $5\hbar$. For both states $J^\pi = 2^-$ and 2^+ , the resulting $\sigma_n^{CN}(E^*, J, \pi)$ have the largest values compared to other negative or positive parities.

B. SP distribution and branching ratio

The $F_{\delta}^{CN}(E^*, J, \pi)$ for $^{234}\text{Pa}^*$ populated by the reaction $^{232}\text{Th}(^3\text{He}, p)^{234}\text{Pa}^*$ is calculated with the DWBA method [38]. The calculated results show that the $F_{\delta}^{CN}(E^*, J, \pi)$ have similar distributions at $E^* = 5.32, 5.52, 5.72, 5.92,$ and 6.12 MeV, which correspond to the experimental measurement points provided in Ref. [10]. Figure 3 shows an exemplary result for $F_{\delta}^{CN}(E^*, J, \pi)$ at $E^* = 5.72$ MeV. It shows that the average spin $\langle J \rangle$ for the $^{234}\text{Pa}^*$ is approximately $3.5\hbar$. This value is larger than the $\langle J \rangle \approx .2\hbar$ for the reaction $^{233}\text{Pa}(n, \gamma)^{234}\text{Pa}^*$, which is obtained with the TALYS (version 1.96) calculations.

Beside the $F_{\delta}^{CN}(E^*, J, \pi)$, the $G_{\gamma}^{CN}(E^*, J, \pi)$ is another ingredient used to obtain the $P_{\delta\gamma}(E^*)$, as shown in Eq. (6). However, in order to calculate the $G_{\gamma}^{CN}(E^*, J, \pi)$, an important prerequisite is to extract reasonably the factor G_{norm} by minimizing the χ^2 discussed above. In our case, a minimum $\chi^2 \approx 3.38$ is obtained and the resulting factor $G_{\text{norm}} = 3.2$. The $G_{\gamma}^{CN}(E^*, J, \pi)$ is readily obtained according to Eqs. (4) and (5). By substituting the $F_{\delta}^{CN}(E^*, J, \pi)$ (see Fig. 3) and the $G_{\gamma}^{CN}(E^*, J, \pi)$ into Eq. (6), the theoretical P_{theo} is finally obtained. When $G_{\text{norm}} = 3.2$, the P_{theo} values obtained at $= 5.32, 5.52, 5.72, 5.92,$ and 6.12 MeV are shown in Fig. 4, together with the experimental P_{exp} . Note that since the P_{theo} have a visible difference with the P_{exp} at $E^* = 5.32$ MeV, the obtained χ^2 is slightly larger than unity in our case.

C. $^{233}\text{Pa}(n, \gamma)$ cross section

The $\sigma_{n\gamma}(E_n)$ extracted with the surrogate reaction $^{233}\text{Pa}(n, \gamma)^{234}\text{Pa}^*$ involving the SP distribution is shown in

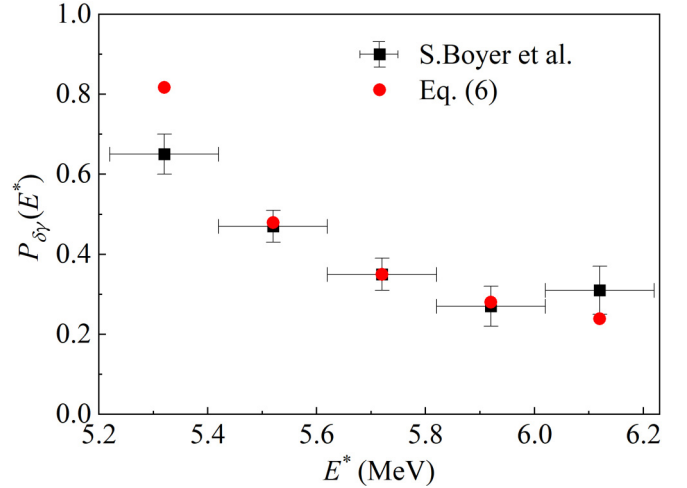


FIG. 4. The calculated and experimental $P_{\delta\gamma}(E^*)$ at $= 5.32, 5.52, 5.72, 5.92,$ and 6.12 MeV. The calculated data are obtained when χ^2 is minimized to be 3.38. The experimental data are taken from Ref. [10].

Fig. 5. For comparison, the experimental data and the available evaluations in ENDF/B-VIII.0 [11], JENDL-5 [12], and ROSFOND-2010 [15] are also shown therein. One can see that the extracted $\sigma_{n\gamma}(E_n)$ decreases with the neutron energy. Besides the ROSFOND-2010 data, the other evaluated and experimental ones show the same decreasing trend. The JENDL-5 evaluations in line with the ENDF/B-VIII.0. The present data considering the SP distribution are in accordance with the ENDF/B-VIII.0 and JENDL-5 evaluations when $E_n \leq 0.3$ MeV, above which they start to deviate from the latter by a factor of less than 0.5. However, the experimental data are at least two times higher than the JENDL-5 and ENDF/B-VIII.0 evaluations when $E_n \geq 0.2$ MeV, as shown in Fig. 5. This is mainly caused by the fact that the SP effect is ignored when calculating the branching ratio for the $^{234}\text{Pa}^* \gamma$

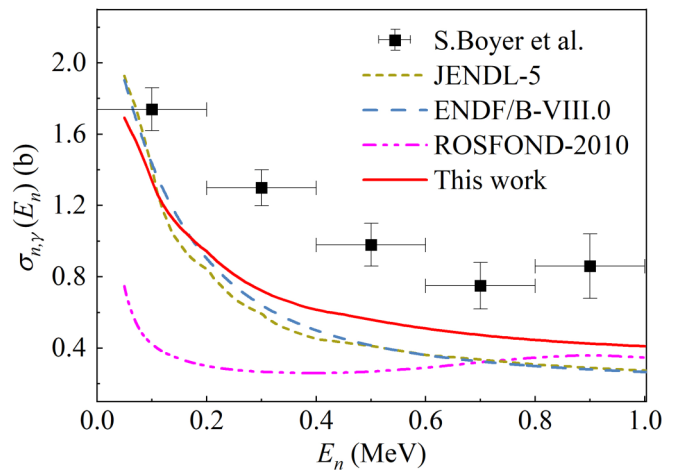


FIG. 5. The $^{233}\text{Pa}(n, \gamma)$ cross section depending on neutron energy. The calculated data are obtained when $G_{\text{norm}} = 3.2$. The experimental data is taken from Ref. [10] and the evaluated ones are taken from ENDF/B-VIII.0, JENDL-5, and ROSFOND-2010.

decay, which seems to be a necessary ingredient for extracting the $^{233}\text{Pa}(n, \gamma)$ cross section. As a result, the SP effect should be considered in a proper way when the surrogate-reaction method is employed to extract the $^{233}\text{Pa}(n, \gamma)$ cross section.

IV. CONCLUSION AND PERSPECTIVES

In the present study, we have extracted successfully the $^{233}\text{Pa}(n, \gamma)$ cross section by using the surrogate reaction $^{232}\text{Th}(^3\text{He}, p)^{234}\text{Pa}^*$ involving spin-parity distribution. This is accomplished by the calculation of the $F_{\delta}^{CN}(E^*, J, \pi)$ using the DWBA method and the modeling of the $G_{\gamma}^{CN}(E^*, J, \pi)$ using proper parameter G_{norm} , which results in a good agreement between the experimental and theoretical γ -decay probability for the surrogate reaction $^{232}\text{Th}(^3\text{He}, p)^{234}\text{Pa}^*$. The extracted cross section for the $^{233}\text{Pa}(n, \gamma)$ is in reasonable agreement with both the ENDF/B-VIII.0 and JENDL-5 evaluation, since the SP effect is taken into account when calculating the

branching ratio for the $^{234}\text{Pa}^* \gamma$ decay. It is suggested that the SP effect would play a key role in extracting the (n, γ) cross section when employing the surrogate-reaction method, which seems to be useful for determining the (n, γ) cross section for those short-lived and unstable nuclei. In the near future, we will employ the surrogate-reaction method involving the SP distribution to study some other interesting cases related to the short-lived nuclei, such as ^{239}Np [39] and ^{241}Am [40].

ACKNOWLEDGMENTS

We thank B. S. Huang for valuable discussions. This work is supported by the National Key R&D Program of China (Grant No. 2022YFA1603300), and the National Natural Science Foundation of China (Grants No. U2230133 and No. U2067205) and the Hengyang Municipal Science and Technology Project (No. 202150054076).

-
- [1] G. Zheng, H. Wu, J. Wang, S. Chen, and Y. Zhang, *Ann. Nucl. Energy* **116**, 177 (2018).
 - [2] J. Serp, M. Allibert, O. Bene, S. Delpech, O. Feynberg, V. Ghetta, D. Heuer, D. Holcomb, V. Ignatiev, J. L. Kloosterman *et al.*, *Prog. Nucl. Energy* **77**, 308 (2014).
 - [3] B. Mignacca and G. Locatelli, *Prog. Nucl. Energy* **129**, 103503 (2020).
 - [4] M. Petit, M. Aiche, G. Barreau, S. Boyer, N. Carjan, S. Czajkowski, D. Dassié, C. Grosjean, A. Guiral, B. Haas *et al.*, *Nucl. Phys. A* **735**, 345 (2004).
 - [5] O. Bringer, H. Isnard, I. AlMahamid, F. Chartier, and A. Letourneau, *Nucl. Instrum. Methods Phys. Res. A* **591**, 510 (2008).
 - [6] J. Halperin, R. W. Stoughton, C. V. Ellison, and D. E. Ferguson, *Nucl. Sci. Eng.* **1**, 1 (1956).
 - [7] J. C. Connor, R. T. Bayard, D. Macdonald, and S. B. Gunst, *Nucl. Sci. Eng.* **29**, 408 (1967).
 - [8] T. A. Eastwood and R. D. Werner, *Can. J. Phys.* **38**, 751 (1960).
 - [9] N. D. Scielzo, J. E. Escher, J. M. Allmond, M. S. Basunia, C. W. Beausang, L. A. Bernstein, D. L. Bleuel, J. T. Harke, R. M. Clark, F. S. Dietrich *et al.*, *Phys. Rev. C* **81**, 034608 (2010).
 - [10] S. Boyer, D. Dassié, J. N. Wilson, M. Aïche, G. Barreau, S. Czajkowski, C. Grosjean, A. Guiral, B. Haas, B. Osmanov *et al.*, *Nucl. Phys. A* **775**, 175 (2006).
 - [11] D. A. Brown, M. B. Chadwick, R. Capote, A. C. Kahler, A. Trkov, M. W. Herman, A. A. Sonzogni, Y. Danon, A. D. Carlson, M. Dunn *et al.*, *Nucl. Data Sheets* **148**, 1 (2018).
 - [12] O. Iwamoto, N. Iwamoto, S. Kunieda *et al.*, *J. Nucl. Sci. Technol.* **60**, 1 (2023).
 - [13] R. Capote, L. Leal, P. Liu, T. Liu, P. Schillebeeckx, M. Sin, I. Sirakov, and A. Trkov, *Evaluated Nuclear Data for Nuclides within the Thorium-Uranium Fuel Cycle*, Non-serial Publications (International Atomic Energy Agency, Vienna, 2010).
 - [14] O. Iwamoto, *J. Nucl. Sci. Technol.* **44**, 687 (2007).
 - [15] S. V. Zabrodskaia, A. V. Ignatyuk, V. N. Koshcheev, V. N. Manochin, M. N. Nikolaev, and V. G. Pronyaev, *Nucl. Constants* **1**, 3 (2007).
 - [16] J. E. Escher and F. S. Dietrich, *Phys. Rev. C* **81**, 024612 (2010).
 - [17] V. F. Weisskopf and D. H. Ewing, *Phys. Rev.* **57**, 472 (1940).
 - [18] J. D. Cramer and H. C. Britt, *Nucl. Sci. Eng.* **41**, 177 (1970).
 - [19] W. Younes and H. C. Britt, *Phys. Rev. C* **67**, 024610 (2003).
 - [20] J. E. Escher, J. T. Harke, F. S. Dietrich, N. D. Scielzo, I. J. Thompson, and W. Younes, *Rev. Mod. Phys.* **84**, 353 (2012).
 - [21] J. E. Escher, J. T. Harke, R. O. Hughes, N. D. Scielzo, R. J. Casperson, S. Ota, H. I. Park, A. Saastamoinen, and T. J. Ross, *Phys. Rev. Lett.* **121**, 052501 (2018).
 - [22] A. Ratkiewicz, J. A. Cizewski, J. E. Escher, G. Potel, J. T. Harke, R. J. Casperson, M. McCleskey, R. A. E. Austin, S. Burcher, R. O. Hughes *et al.*, *Phys. Rev. Lett.* **122**, 052502 (2019).
 - [23] R. Pérez Sánchez, B. Jurado, V. Méot, O. Roig, M. Dupuis, O. Bouland, D. Denis-Petit, P. Marini, L. Mathieu, I. Tsekhanovich *et al.*, *Phys. Rev. Lett.* **125**, 122502 (2020).
 - [24] N. Bohr, *Nature (London)* **137**, 344 (1936).
 - [25] W. Hauser and H. Feshbach, *Phys. Rev.* **87**, 366 (1952).
 - [26] J. Hüfner, C. Mahaux, and H. A. Weidenmüller, *Nucl. Phys. A* **105**, 489 (1967).
 - [27] D. Y. Pang, P. Roussel-Chomaz, H. Savajols, R. L. Varner, and R. Wolski, *Phys. Rev. C* **79**, 024615 (2009).
 - [28] A. J. Koning and J. P. Delaroche, *Nucl. Phys. A* **713**, 231 (2003).
 - [29] I. Brida, S. C. Pieper, and R. B. Wiringa, *Phys. Rev. C* **84**, 024319 (2011).
 - [30] R. Capote, M. Herman, P. Obložinský, P. G. Young, S. Goriely, T. Belgia, A. V. Ignatyuk, A. J. Koning, S. Hilaire, V. A. Plujko *et al.*, *Nucl. Data Sheets* **110**, 3107 (2009).
 - [31] A. Gilbert and A. G. W. Cameron, *Can. J. Phys.* **43**, 1446 (1965).
 - [32] G. N. Smirenkin, Preparation of evaluated data for a fission barrier parameter library for isotopes with $z=82-98$, with consideration of the level density models used (1993).
 - [33] J. Kopecky and M. Uhl, *Phys. Rev. C* **41**, 1941 (1990).
 - [34] S. Goriely, S. Hilaire, S. Péru, and K. Sieja, *Phys. Rev. C* **98**, 014327 (2018).

- [35] B. L. Berman and S. C. Fultz, *Rev. Mod. Phys.* **47**, 713 (1975).
- [36] P. Carlos, R. Bergère, H. Beil, A. Leprêtre, and A. Veyssièrè, *Nucl. Phys. A* **219**, 61 (1974).
- [37] A. J. Koning and D. Rochman, *Nucl. Data Sheets* **113**, 2841 (2012).
- [38] I. J. Thompson, *Comput. Phys. Rep.* **7**, 167 (1988).
- [39] O. Shcherbakov, K. Furutaka, S. Nakamura, H. Sakane, K. Kobayashi, S. Yamamoto, J. Hori, and H. Harada, *J. Nucl. Sci. Technol.* **42**, 135 (2005).
- [40] E. Mendoza, D. Cano-Ott, C. Guerrero, S. Altstadt, J. Andrzejewski, L. Audouin, M. Barbagallo, V. Bécàres, F. Bečvář, F. Belloni *et al.*, *Nucl. Data Sheets* **119**, 65 (2014).